AIMS Mathematics, 9(7): 19397–19413.
DOI: 10.3934/math.2024945
Received: 12 April 2024
Revised: 21 May 2024
Accepted: 3 June 2024
Published: 12 June 2024

https://www.aimspress.com/journal/Math

Research article

The asymptotic spreading speeds of COVID-19 with the effect of delay and quarantine

Khalaf M. Alanazi*

Department of Mathematics, College of Science, Northern Border University, Arar, Saudi Arabia

* **Correspondence:** Email: Khalaf.Mtr@nbu.edu.sa.

Abstract: Coronavirus spread in Wuhan, China, in December 2019. A few weeks later, the virus was present in over 100 countries around the globe. Governments have adopted extreme measures to contain the spreading virus. Quarantine is considered the most effective way to control the spreading speed of COVID-19. In this study, a mathematical model is developed to explore the influence of quarantine and the latent period on the spatial spread of COVID-19. We use the mathematical model with quarantine, and delay to predict the spreading speed of the virus. In particular, we transform the model to a single integral equation and then apply the Laplace transform to find implicit equations for the spreading speeds. The basic reproduction number of COVID-19 is also found and calculated. Numerical simulations are performed to confirm our theoretical results. To validate the proposed model, we compare our outcomes with the actual reported data published by the National Health Commission of China and the Health Commission of local governments. The model demonstrates good qualitative agreement with the actual data reported. The results show that delay and quarantine highly influence the spreading speeds of COVID-19. Also, we can only contain the disease if we quarantine 75% of the infected people.

Keywords: COVID-19; epidemic model; spreading speed; quarantine; delay model; numerical simulation
Mathematics Subject Classification: 92D30, 45K05

1. Introduction

A severe acute respiratory syndrome coronavirus 2 (SARS-COV-2) spread in Wuhan, China, in December 2019. The novel coronavirus disease has been called COVID-19 by the World Health Organization (WHO) [5]. As of Jan 29, 2020, there were 5993 confirmed cases in China and 132 reported deaths [44]. The numbers increased rapidly to over 77,500 confirmed cases and 2600 deaths as of Feb 24, 2020 [30]. The National Health Commission of China and the Health Commission of

local governments report daily the number of new disease cases and their locations. Here, we care about the data reported by these Commissions and by Feng et al. [19] from Jan 17, 2020 to Mar 20, 2020. The results [19, Figure 1] show that the disease outbreak began in Wuhan, and no cases were reported in any other region of the country until Jan 17, 2020. The government of China imposed a lockdown on Wuhan on Jan 23 [19]. The number of cases peaked on February 7 according to [19], and on February 10 according to [14]. The COVID-19 virus was able to spread to other cities despite the government's efforts to control the disease. By the end of February 2020, the number of new cases reported was gradually slowing down [19]. This indicates that the COVID-19 virus was under control within two months [19, Figure 1].

The value of the basic reproduction number is significant in pathology. The basic reproduction number is the average number of people catching a disease from one infectious person [13]. At the early stages of the epidemic in China, the basic reproduction number has been reported between 2 to 3.58 [20, 22, 24, 27, 28, 30–32, 42, 44, 46]. Other authors estimated the mean value of the basic reproduction number to be from 4.8 to 7.08 [5, Figure 1].

Governments have adopted extreme measures, such as social distancing, quarantine, and travel restrictions to minimize the spread of the virus. About a week after applying some of these measures, the basic reproduction number dropped to 1.05 [27]. According to [23], quarantine is the most effective way to contain the disease.

Because of the direct impact of COVID-19 on global health, many mathematical models and studies have been published, see [5, 6, 12, 14, 18, 19, 21, 23, 24, 27, 29, 36, 41, 43, 44, 47]. The current COVID-19 mathematical models are mostly a system of ordinary differential equations [5, 6, 12, 18, 21, 24, 27, 29, 44]. For mathematical models that consider quarantine and isolation measures, we refer to [14, 23, 34]. [11] developed a SEIR model to describe the interactions between passengers and crews on a ship and the influence of quarantine to slow the spread of the disease. [14] introduced a model for COVID-19 to investigate the power of isolation and quarantine further. The mathematical model in [47] assumes that individuals are quarantined during the infected or infectious stage. In contrast, the mathematical models in [10, 26, 35] suggest a possible quarantine for susceptible, infected, and infectious individuals.

Due to the incubation period of COVID-19, infected individuals are subject to some time delay before being transferred to the infectious state. The model we study in this paper describes the infected individuals in the latent period, which makes it more appropriate to investigate the spatial dynamics of COVID-19. Recently, modeling the infection age is more common, and this leads to more complicated mathematical models, see [36, 39]. The incubation period ranges from 1 to 14 days [13]. The mean incubation period is three days in [30], from 5 to 6.4 in [42,45]. The mean length of infectious periods is five days in [30] and 1.61 days in [31]. The latent and incubation periods are assumed to be exact [44].

Hence, we propose a model with a time delay due to the incubation period to understand the dynamics of COVID-19 better. Also, we study the influence of quarantine and the values of the parameters on the spatial spreading speeds of COVID-19 in China. This can be done by applying the concept of asymptotic speeds of the spread of an epidemic discussed by Diekmann [15–17] and Thieme [37, 38], generalized by Thieme and Zhao [40], and applied recently by Alanazi, Jackiewicz, and Thieme [2, 4].

According to Diekmann [16, 17] and Thieme [37, 38], an epidemic can be described by

$$u(t,x) = u_0(t,x) + \int_0^t \int_{\mathbb{R}^n} G(u(t-s, x-y), s, y)dyds,$$

if there is no increase in the susceptible individuals by birth, immigration, or recovery. In this equation, u is the cumulative rate of infected individuals meeting the susceptible, which describes the development of the population. The initial conditions are collected and listed in u_0. The nonlinear term G contains integral kernels that measure the contribution of infected individuals to the cumulative rate u. Aronson and Weinberger [8, 9] and Aronson [7] show that c^* is called the asymptotic speed if the solution u converges to zero uniformly when $|x| \geq ct$ for $c > c^*$, whereas it is bounded away from zero uniformly when $|x| \leq ct$ for $c < c^*$ after a sufficiently long time t. For more on this, we refer to the work by Ruan [33].

The paper is organized as follows. In Section 2, we consider a mathematical model with quarantine and a generally distributed length of the incubation stage. In Section 3, we reduce the model to a single integral equation where the theory of asymptotic speeds of spread can apply. The definition of the spreading speeds and the basic reproduction number are also introduced in Section 3. Numerical examples are given in Section 4 to confirm some of the analytic findings. The theoretical and numerical results are discussed in Section 5.

2. COVID-19 model with delay and quarantine

The model assumes the infected individuals of COVID-19 are not infectious during the incubation stage, see [20, 44]. Also, quarantining all of the infectious population is not possible. Therefore, we assume that part of the infectious population is non-quarantined.

Let the density of susceptible individuals be denoted by $S(x,t)$, the density of infected individuals in the latent period be $I(x,a,t)$ with infection age a, and the density of non-quarantined infectious individuals be $Q(x,t)$. Also, let the infected individuals with infection age $a \in [0,\infty)$ leave the latent period with rate $\ell(a)$. Then, the model takes the form

$$\begin{cases} \partial_t S(x,t) &= -\eta S(x,t)Q(x,t), \\ \partial_t Q(x,t) &= (1-\gamma)\int_0^\infty \ell(a)I(x,t,a)da - qQ(x,t), \\ \partial_t I(x,a,t) &+ \partial_a I(x,a,t) = -\ell(a)I(x,a,t), \\ I(x,0,t) &= \eta S(x,t)Q(x,t), \end{cases} \tag{2.1}$$

with $x \in \mathbb{R}^n$ and $t > 0$. The initial densities are

$$S(x,0) = S_0(x),\ I(x,a,0) = I_0(x,a),\ Q(x,0) = Q_0(x). \tag{2.2}$$

$\eta > 0$ is the disease transmission coefficient, and $\ell > 0$ is the per capita transition rate from the latent (infected) stage to the infectious stage. ℓ is a continuous function and ℓ: $[0,\infty) \to [0,\infty)$. The effectiveness of quarantine is given by γ, where $1 > \gamma \geq 0$. $1/q > 0$ is the mean length of the infectious period. We assume that the initial are nonnegative continuous functions.

We reduce system (2.1) by integrating along the characteristics for the infected individuals $I(x,a,t)$. Let $a = t + r$, $i_r(x,t) = I(x,t+r,t)$, and $t_r = \max\{0,-r\}$, where $r \in \mathbb{R}$. Then, the model of infected

individuals inside the latent period becomes

$$\begin{cases} \partial_t i_r(x,t) = -\ell(t+r) i_r(x,t), \\ i_r(x,t_r) = I(x,t_r+r,t_r), \end{cases}$$

for $t \geq t_r$. Solving, we get

$$i_r(x,t) = i_r(x,t_r) e^{-\int_{t_r}^{t} \ell(s+r)ds}.$$

Therefore, for $a > t$,

$$i_r(x,t) = i_r(x,0) e^{-\int_0^t \ell(s+r)ds}.$$

Let $s \to s-r$. Then we get

$$i_r(x,t) = i_r(x,0) \frac{e^{-\int_0^{t+r} \ell(s)ds}}{e^{-\int_0^r \ell(s)ds}}.$$

Let $L(r) = \exp\left(-\int_0^r \ell(s)ds\right)$. Then we conclude

$$i_r(x,t) = i_r(x,0) \frac{L(t+r)}{L(r)}. \tag{2.3}$$

For $t > a$,

$$i_r(x,t) = i_r(x,-r) e^{-\int_{-r}^{t} \ell(s+r)ds}.$$

Also, let $s \to s-r$. Then we have

$$i_r(x,t) = i_r(x,-r) e^{-\int_0^{t+r} \ell(s)ds} = i_r(x,-r) L(t+r). \tag{2.4}$$

Therefore, from (2.3), we have

$$I(x,a,t) = I_0(x,a-t) \frac{L(a)}{L(a-t)}, \qquad a > t \geq 0, \tag{2.5}$$

and from (2.4) we have

$$I(x,a,t) = \eta S(x,t-a) Q(x,t-a) L(a), \qquad t > a \geq 0. \tag{2.6}$$

Substituting (2.5) and (2.6) into (2.1) gives the following system with delay and Volterra integral equations

$$\begin{cases} \partial_t S(x,t) &= -\eta S(x,t) Q(x,t), \\ \partial_t Q(x,t) &= (1-\gamma)\Big(W_1 + W_2\Big) - qQ(x,t), \end{cases} \tag{2.7}$$

where

$$\begin{cases} W_1 &= \eta \int_0^t \ell(a) S(x,t-a) Q(x,t-a) L(a) da, \\ W_2 &= \int_t^\infty \ell(a) \hat{L}(a,t) I_0(x,a-t) da, \end{cases} \tag{2.8}$$

$x \in \mathbb{R}^n$, $t > 0$, and $\hat{L}(a,t) = \frac{L(a)}{L(a-t)}$. We define $L(a) = \exp\left(-\int_0^a \ell(s)ds\right)$ to be the probability that infected individuals with infection age a are still in the latent period. Therefore, L is a decreasing function, $L : \mathbb{R}_+ \to [0,1]$, and $L(0) = 1$.

3. Spreading speeds of COVID-19

Models 2.7 and 2.8 could be reduced to a single integral equation. We begin this section by integrating the differential equations in (2.7). Therefore, we have

$$S(x,t) = S_0(x)e^{-w(x,t)}, \tag{3.1}$$

where

$$w(x,t) = \eta\int_0^t Q(x,r)dr, \tag{3.2}$$

and

$$Q(x,t) = (1-\gamma)\int_0^t e^{-qs}\Big(W_1(x,t-s)+W_2(x,t-s)\Big)ds + Q_0(x)e^{-qt}. \tag{3.3}$$

We substitute (2.8) into (3.3) and do a change of variables several times, and we get the following non-linear equation describing the development of the infectious population,

$$w(x,t) = \eta(1-\gamma)\int_0^t\int_0^r e^{-qs}\ell(r-s)L(r-s)S_0(x)\Big(1-e^{-w(x,t-r)}\Big)dsdr + \hat{w}(x,t), \tag{3.4}$$

where

$$\begin{aligned}\hat{w}(x,t) &= \eta(1-\gamma)\int_0^t\int_0^r\int_0^\infty e^{-qs}\ell(a+r-s)\hat{L}(a+r-s,r-s)I_0(x,a)dadsdr\\ &+ \eta\int_0^t Q_0(x)e^{-qr}dr.\end{aligned} \tag{3.5}$$

Let $\jmath(x,r) = \eta(1-\gamma)\int_0^r e^{-qs}\ell(r-s)L(r-s)S_0(x)ds$. Then, (3.4) becomes

$$w(x,t) = \int_0^t \jmath(x,r)\Big(1-e^{-w(x,t-r)}\Big)dr + \hat{w}(x,t). \tag{3.6}$$

We assume that the initial number of susceptible is constant, then apply one side Laplace transform,

$$\begin{aligned}\mathcal{L}(c,\lambda) &= \int_0^\infty e^{-\lambda cr}\jmath(r)dr,\\ &= \eta(1-\gamma)S_0\int_0^\infty\int_0^r e^{-\lambda cr}e^{-qs}\ell(r-s)L(r-s)dsdr.\end{aligned}$$

We do a change of variables, let $r-s\to r$, and obtain

$$\begin{aligned}\mathcal{L}(c,\lambda) &= \eta(1-\gamma)S_0\int_0^\infty\int_0^\infty e^{-\lambda c(s+r)}e^{-qs}\ell(r)L(r)dsdr,\\ &= \eta(1-\gamma)S_0\int_0^\infty \ell(r)L(r)e^{-\lambda cr}dr\int_0^\infty e^{(-q-\lambda c)s}ds.\end{aligned}$$

We know that $-L'(r) = \ell(r)L(r)$, so we have

$$\mathcal{L}(c,\lambda) = \frac{S_0\eta(1-\gamma)}{q+\lambda c}\int_0^\infty -L'(r)e^{-\lambda cr}dr. \tag{3.7}$$

By the assumptions in Section 2, we have

$$\mathcal{L}(c,\lambda) = \frac{-S_0\eta(1-\gamma)}{q+\lambda c}\int_0^\infty e^{-\lambda cr}dL(r). \tag{3.8}$$

By [40], we can use the Laplace transform to find equations for the spreading speeds c^* as follows:

$$\mathcal{L}(c^*,\lambda) = 1, \qquad \frac{\partial}{\partial\lambda}\mathcal{L}(c^*,\lambda) = 0. \tag{3.9}$$

Example 3.1. Let ρ be the mean length of the incubation period. If the incubation stage is uniformly distributed,

$$L(a) = \begin{cases} 1 - \frac{a}{\rho}, & 0 \le a \le \rho, \\ 0, & a > \rho, \end{cases} \tag{3.10}$$

and then

$$-\int_0^\infty e^{-\lambda ca} dL(a) = \frac{1}{\rho}\int_0^\rho e^{-\lambda ca} da = \frac{1}{\lambda c\rho}\Big[1 - e^{-\lambda c\rho}\Big].$$

Therefore,

$$\mathcal{L}(c,\lambda) = \Big(\frac{1}{\lambda c\rho}\Big)\frac{S_0\eta(1-\gamma)}{q+\lambda c}\Big[1 - e^{-\lambda c\rho}\Big]. \tag{3.11}$$

The basic reproduction number of COVID-19 can be found by replacing λ and c in (3.8) with zero, see [38, 40]. Therefore, the basic reproduction number of COVID-19 is given by

$$\mathcal{R}_0 = \mathcal{L}(0,0) = \frac{S_0\eta(1-\gamma)}{q}\int_0^\infty dL(r). \tag{3.12}$$

According to [16, 17, 38], the spreading speed is defined by

$$c^* := \inf\{c \ge 0;\ \ \exists\lambda > 0 :\ \mathcal{L}(c,\lambda) < 1\}, \tag{3.13}$$

as long as $\mathcal{R}_0 > 1$, and $c^* := 0$ if $\mathcal{R}_0 \le 1$. Therefore, we have the following results.

Theorem 3.2. *Assume the initial conditions I_0 and Q_0 are defined as $I_0(x,a), Q_0(x) \le \varepsilon e^{-\lambda|x|}$, and $|\, x \,| \ge ct$. Then $\hat{w}(x,t) \to 0$ as $t \to \infty$.*

Proof. $\hat{w}(x,t)$ is given in (3.5). Since $\hat{L}(a,t) = \frac{L(a)}{L(a-t)}$, we have

$$\begin{aligned} \hat{w}(x,t) &= -\eta(1-\gamma)\int_0^t\int_0^r\int_0^\infty e^{-qs}L'(a+r-s)I_0(x,a)\tfrac{1}{L(a)}dadsdr \\ &+ \eta\int_0^t Q_0(x)e^{-qr}dr. \end{aligned} \tag{3.14}$$

We change the order of integration as follows:

$$\begin{aligned} \hat{w}(x,t) &= \eta(1-\gamma)\int_0^t\int_0^\infty e^{-qs}\Big[\int_0^{t-s} -L'(a+r-s)dr\Big]I_0(x,a)\tfrac{1}{L(a)} \\ &\quad dads + \eta\int_0^t Q_0(x)e^{-qr}dr, \\ &= \eta(1-\gamma)\int_0^t\int_0^\infty e^{-qs}\Big[L(a) - L(a+t-s)\Big]I_0(x,a)\tfrac{1}{L(a)} \\ &\quad dads + \eta\int_0^t Q_0(x)e^{-qr}dr, \\ &\le \eta(1-\gamma)\int_0^t\int_0^\infty e^{-qs}I_0(x,a)dads + \eta\int_0^t Q_0(x)e^{-qr}dr. \end{aligned}$$

By the assumptions $I_0(x,a), Q_0(x) \le \varepsilon e^{-\lambda|x|}$, we have

$$\begin{aligned} \hat{w}(x,t) &\le \varepsilon\eta(1-\gamma)e^{\lambda(ct-|x|)}\int_0^t e^{s(-\lambda c-q)}ds + \varepsilon\eta e^{\lambda(ct-|x|)}\int_0^t e^{r(-\lambda c-q)}dr, \\ &= \tfrac{(2\varepsilon\eta-\gamma\varepsilon\eta)}{\lambda c+q}e^{\lambda(ct-|x|)}. \end{aligned}$$

Since $\gamma < 1$ and $|\, x \,| \ge ct$, $\hat{w}(x,t) \to 0$ as $t \to \infty$. This completes the proof. □

Theorem 3.3. *Let $\hat{\rho} > 0$ be the minimum length of the latent period, L_1 be a decreasing function such that $L_1 : \mathbb{R}_+ \to [0, 1]$, and $L(a)$ be defined as*

$$L(r) = \begin{cases} 1, & 0 \le r < \hat{\rho}, \\ L_1(r - \hat{\rho}), & \hat{\rho} < r < \infty. \end{cases} \tag{3.15}$$

Then:
(1) $\mathcal{L}(c, \lambda) \le \frac{S_0\eta(1-\gamma)}{q+\lambda c} e^{-\lambda c\hat{\rho}}$.
(2) $\mathcal{L}(c, \lambda) \to \frac{S_0\eta(1-\gamma)}{q+\lambda c}$ *as* $\hat{\rho} \to 0$.
(3) $\mathcal{L}(c, \lambda) \to 0$ *as* $\hat{\rho} \to \infty$, *which provides* $c^* \le c$.
(4) $\mathcal{L}(c, \lambda) \to \mathcal{R}_0$ *as* $\lambda \to 0$.

Proof. (1) By (3.7),

$$\mathcal{L}(c, \lambda) = \frac{S_0\eta(1-\gamma)}{q+\lambda c} \int_0^\infty -L'(r)e^{-\lambda cr} dr.$$

The integration by parts of $\int_0^\infty -L'(r)e^{-\lambda cr} dr$ gives

$$\mathcal{L}(c, \lambda) = \frac{S_0\eta(1-\gamma)}{q+\lambda c}\Big(1 - \lambda c \int_0^\infty L(r)e^{-\lambda cr} dr\Big), \text{ [39]}.$$

From the definition in (3.15), we get

$$\begin{aligned} \mathcal{L}(c, \lambda) &= \frac{S_0\eta(1-\gamma)}{q+\lambda c}\Big(1 - \lambda c \int_0^{\hat{\rho}} e^{-\lambda cr} dr - \lambda c \int_{\hat{\rho}}^\infty L_1(r - \hat{\rho})e^{-\lambda cr} dr\Big), \\ &= \frac{S_0\eta(1-\gamma)}{q+\lambda c}\Big(e^{-\lambda c\hat{\rho}} - \lambda c \int_{\hat{\rho}}^\infty L_1(r - \hat{\rho})e^{-\lambda cr} dr\Big). \end{aligned}$$

Let $r - \hat{\rho} \to r$. Then we have

$$\begin{aligned} \mathcal{L}(c, \lambda) &= \frac{S_0\eta(1-\gamma)}{q+\lambda c}\Big(e^{-\lambda c\hat{\rho}} - \lambda c e^{-\lambda c\hat{\rho}} \int_0^\infty L_1(r)e^{-\lambda cr} dr\Big), \\ &= \frac{S_0\eta(1-\gamma)}{q+\lambda c} e^{-\lambda c\hat{\rho}}\Big(1 - \lambda c \int_0^\infty L_1(r)e^{-\lambda cr} dr\Big). \end{aligned}$$

Therefore,

$$\mathcal{L}(c, \lambda) \le \frac{S_0\eta(1-\gamma)}{q+\lambda c} e^{-\lambda c\hat{\rho}}. \tag{3.16}$$

(2) By (3.16), $\mathcal{L}(c, \lambda) \to \frac{S_0\eta(1-\gamma)}{q+\lambda c}$ as $\hat{\rho} \to 0$.
(3) By (3.16), $\mathcal{L}(c, \lambda) \to 0$ as $\hat{\rho} \to \infty$. By definition (3.13), we conclude $c^* \le c$.
(4) We clearly have $\mathcal{L}(c, \lambda) \to \mathcal{R}_0$ as $\lambda \to 0$ from (3.16). □

Theorem 3.4. *Let $L(a)$ be defined as in (3.10). Then, $\mathcal{L}(c, \lambda) \to 0$ as $\lambda \to \infty$. Also, $\mathcal{L}(c, \lambda) \to 0$ as $\rho \to \infty$.*

Proof. By (3.11),

$$\begin{aligned} \mathcal{L}(c, \lambda) &= \Big(\frac{1}{\lambda c\rho}\Big)\frac{S_0\eta(1-\gamma)}{q+\lambda c}\Big[1 - e^{-\lambda c\rho}\Big], \\ &\le \Big(\frac{1}{\lambda c\rho}\Big)\frac{S_0\eta(1-\gamma)}{q+\lambda c}. \end{aligned}$$

This shows $\mathcal{L}(c, \lambda) \to 0$ by either $\lambda \to \infty$ or $\rho \to \infty$. □

Theorem 3.5. *The spreading speed c^* of COVID-19 is an increasing function of S_0 and η.*

Proof. The Laplace transform $\mathcal{L}(c, \lambda)$ is an increasing function of S_0, η, and d for all $c, \lambda > 0$. By [4, Corollary 8.2], the associated spreading speeds are also increasing functions of these parameters. □

Theorem 3.6. *The spreading speed c^* of COVID-19 is a decreasing function with the effectiveness of quarantine γ and q.*

Proof. Since the Laplace transform $\mathcal{L}(c, \lambda)$ is a decreasing function with the effectiveness of quarantine γ and q for all $c, \lambda > 0$, the assertion holds by [4, Corollary 8.2]. □

4. Numerical experiments

4.1. Numerical approximations of the basic reproduction number $\mathcal{R}_0$ of COVID-19

By (3.12), the basic reproduction number of COVID-19 is

$$\mathcal{R}_0 = \frac{S_0\eta(1-\gamma)}{q}\int_0^\infty dL(r). \tag{4.1}$$

Therefore, the disease is going to spread as long as $\mathcal{R}_0 > 1$. With the given values in Table 1, the threshold density of the susceptible at which $\mathcal{R}_0 = 1$ is $S_0^T \approx 1.05[\text{people/km}^2]$ for $\gamma = 0$. The values of $\mathcal{R}_0$ at different values of S_0 are demonstrated in Table 2.

Table 1. Values of the model parameters.

Parameter	Biological meaning	Units	Values	References
η	Disease transmission coefficient	[km^2/day]	0.59	[30]
ρ	The incubation period value	[day]	3	[30]
$1/q$	The mean length of infectious period	[day]	1.61	[31]

Table 2. Values of $\mathcal{R}_0$ at different values of the initial susceptible density S_0. The numerical values of the parameters are given in Table 1.

S_0	$\mathcal{R}_0$ when $\gamma = 0$	$\mathcal{R}_0$ when $\gamma = 0.5$
1	0.9499	0.4750
2	1.8998	0.9499
3	2.8497	1.424
4	3.7996	1.8998
5	4.7495	2.3748
7	6.6493	3.3247
9	8.5491	4.2745

4.2. Propagation of COVID-19

Assuming that the infected individuals leave the latent period with fixed rate ρ such that $\ell(a)$ is one for $0 \leq a < \rho$ and zero otherwise. Then, the model takes the form,

$$\begin{cases} \partial_t S(x,t) &= -\eta S(x,t)Q(x,t), \\ \partial_t Q(x,t) &= (1-\gamma)I(x,t,\rho) - qQ(x,t), \\ \partial_t I(x,a,t) &+ \partial_a I(x,a,t) = -\ell(a)I(x,a,t), \\ I(x,0,t) &= \eta S(x,t)Q(x,t), \end{cases} \tag{4.2}$$

where $x \subseteq \mathbb{R}$ and $t \in [0, 60]$ is measured in days. The initial densities have been selected as follows:

$$S(x,0) = 10,\ I(x,a,0) = 0,\ Q(x,0) = 3e^{-|x|}. \tag{4.3}$$

Systems (4.2) and (4.3) are discretized in space. Then, we apply the continuous Runge-Kutta method of the fourth-order and the discrete Runge-Kutta method of the third-order to approximate the solutions in time. This numerical method provides accurate and stable solutions, as discussed in [2, 3]. The dynamics of (4.2) and (4.3) are presented in Figures 1–4. The approximated solutions of the density of susceptible $S(x,t)$ are demonstrated in Figure 1, and the approximated solutions of the density of non-quarantined infectious individuals $Q(x,t)$ are shown in Figure 2. The contour plots of S and Q are depicted in Figures 3 and 4. The numerical values of the parameters are chosen from the literature as in Table 1.

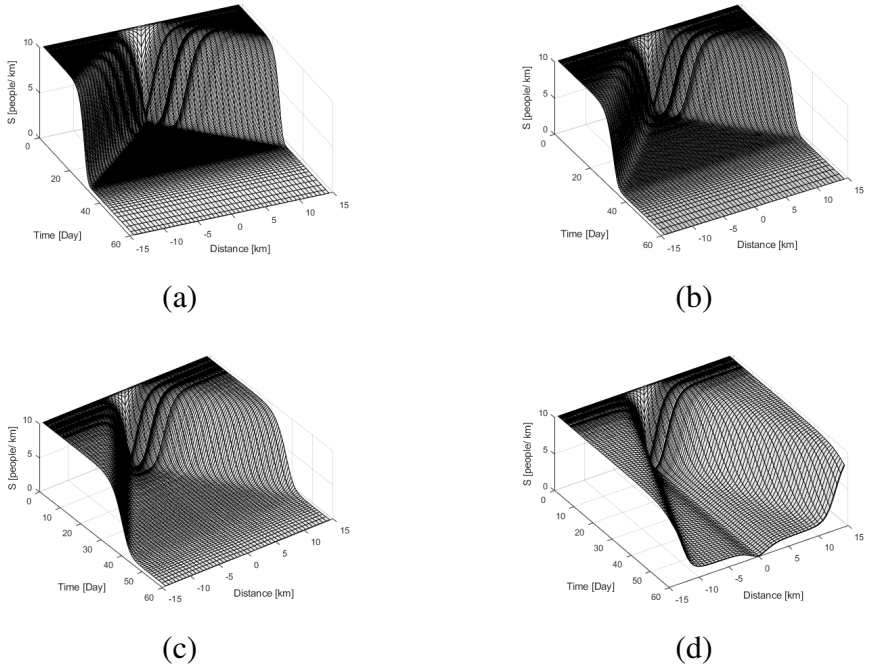

Figure 1. Plots of $S(x,t)$ at different values of quarantine. (a) $\gamma = 0$, (b) $\gamma = 0.25$, (c) $\gamma = 0.50$, (d) $\gamma = 0.75$.

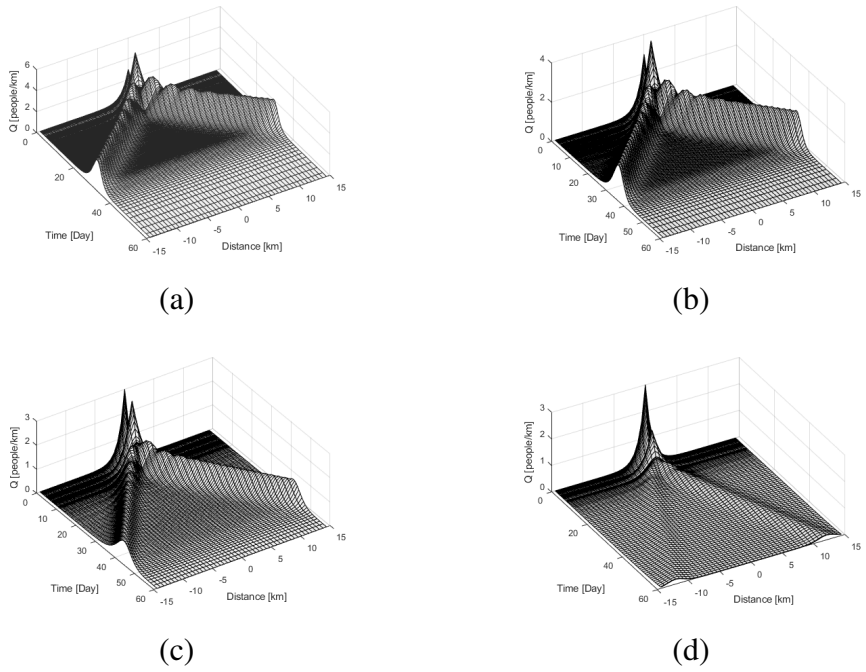

Figure 2. Plots of $Q(x,t)$ at different values of quarantine. (a) $\gamma = 0$, (b) $\gamma = 0.25$, (c) $\gamma = 0.50$, (d) $\gamma = 0.75$.

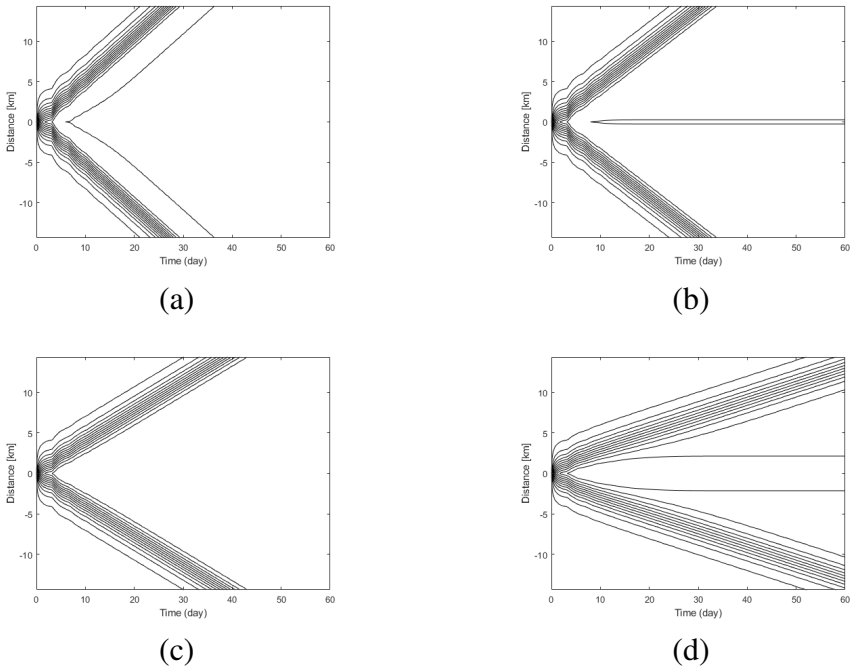

Figure 3. Contour plots of $S(x,t)$ at different values of quarantine. (a) $\gamma = 0$, (b) $\gamma = 0.25$, (c) $\gamma = 0.50$, (d) $\gamma = 0.75$.

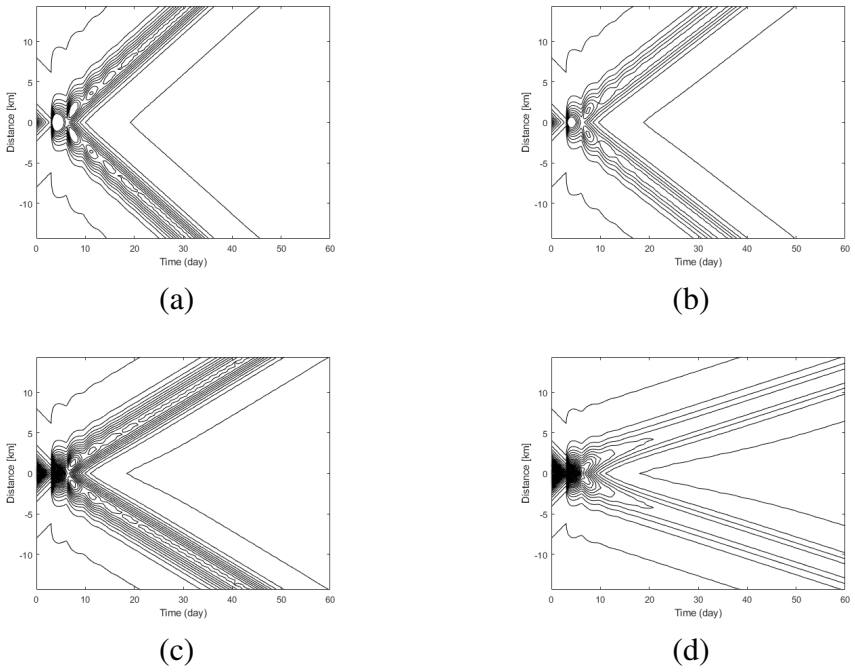

Figure 4. Contour plots of $Q(x,t)$ at different values of quarantine. (a) $\gamma = 0$, (b) $\gamma = 0.25$, (c) $\gamma = 0.50$, (d) $\gamma = 0.75$.

5. Discussion

In this work, we present a mathematical model with time delay and quarantine to study the dynamics of COVID-19. We aim to investigate the influence of the latent period, quarantine, and the values of the parameters on the spatial spreading speeds of COVID-19 in China. We reduce the model to a single equation so that the concept of asymptotic speeds of the spread of an epidemic can be used. In the other part of this work, we provide a numerical simulation to assess our proposed model.

The dynamics of COVID-19 are presented in Figures 1–4. Figure 3 depicts contour plots of the density of susceptible individuals $S(x,t)$, while Figure 4 displays contour plots of the density of non-quarantined infectious individuals $Q(x,t)$. The contour plots in Figures 3 and 4 are essential to predict the spatial spreading speeds of COVID-19. Figure 1 demonstrates the dynamics of the density of susceptible individuals $S(x,t)$, while Figure 2 exhibits the density of non-quarantined infectious individuals $Q(x,t)$ for different scenarios. In the first scenario, we assume that there are no quarantines imposed by the government of China, i.e., $\gamma = 0$. This choice depicts massive waves in the density of non-quarantined infectious individuals $Q(x,t)$ and huge drops in the density of susceptible individuals $S(x,t)$. Increasing the chance of quarantining infected individuals by 25% leads to a considerable decrease in the spreading speeds of COVID-19 as in Figures 1(b) and 2(b). Increasing the quarantine rate to 50% of the infected individuals shows that the first wave of COVID-19 would not hit the boundaries until about 45 days after the pandemic began. The last scenario shows that the disease is under control within two months if we can quarantine 75% of the infected people. The actual data published by the National Health Commission of China and the Health Commission of local governments during the period from Jan 17, 2020, to Mar 20, 2020,

demonstrate that the cumulative number of infected people peaked after twenty days, which is on Feb 7, 2020 [19]. To reduce the spreading speed of the virus, the government of China imposed a lockdown in Wuhan on Jan 23 [19]. The data reported by the National Health Commission of China and the Health Commission of local governments show that the disease of COVID-19 was under control within two months [19, Figure 1]. Therefore, the model demonstrates good qualitative agreement with the actual data published by the National Health Commission of China and the Health Commission of local governments, and is summarized by [19, Figure 1]. This study shall help experts and decision-makers understand the spatial spreading speeds of COVID-19 better and make the necessary efforts to prevent the virus from spreading further.

The numerical results displayed in Table 3–6 are consistent with the analytic results in Theorems 3.5 and 3.6. The spreading speeds of COVID-19 that are given in Tables 3–6 are summarized in Table 7. Tables 3 and 4 indicate that c^* is an increasing function of the initial number of susceptible S_0 and the disease transmission coefficient η (Theorem 3.5), while Tables 3 and 6 demonstrates that the spreading speeds of COVID-19 is a decreasing function with the effectiveness of quarantine γ and with the mean length of the infectious period $1/q$ (Theorem 3.6). Table 5 depicts c^* as a decreasing function with the mean length of the incubation period ρ. Alanazi [1] studied the asymptotic spreading speeds of COVID-19 by assuming that the susceptible, infected, and infectious individuals can diffuse by adding the diffusing coefficients to the model. The results are demonstrated in Table 8 [1, Table 2]. The results demonstrated in Table 8 depict that the diffusion coefficients greatly impact the disease's spreading speed. Overall, the values of the model parameters can highly influence the spreading speeds of COVID-19. Also, Figures 1 and 2 suggest that $S(x,t) \to S_0$ and $Q(x,t) \to 0$ as $\gamma \to 1$, which clearly show that quarantine measures are constructive and effective in containing the disease.

It is feasible to show that the assumptions of Theorem 2.1 in [40] hold. Therefore, since $\hat{w}(x,t) \to 0$ as $t \to \infty$ (Theorem 3.2), we have $w(x,t) \to 0$ as $t \to \infty$ for $| x | \geq ct$ and $c > c^*$. This shows that if you move away from any point in $\mathbb{R}$ for sufficiently large t with speed c that is higher than the minimal speed c^*, then you would be able to outrun the infected population. However, the infected population will surpass you if $c < c^*$.

The basic reproduction number has been calculated to be between 2 and 3.58 [20, 22, 24, 25, 27, 28, 30–32, 42, 44, 46]. The calculated range of $\mathcal{R}_0$ means that one patient could infect two to three other people [42]. We can reach the following conclusions by Table 2. First, the range $\mathcal{R}_0 \in [2, 3.58]$ suggests that the density of susceptible individuals S_0 available to be infected is from approximately 2 [people/km^2] to 4 [people/km^2]. In addition, S_0 greatly impacts the value of the basic reproduction number $\mathcal{R}_0$. Quarantining part of the infectious population can effectively reduce the value of $\mathcal{R}_0$ as demonstrated by Table 2. This clearly shows that population density and quarantine play crucial roles in the spreading speed of COVID-19.

Table 3. Calculated c^* [km/week] at different values of γ. The numerical values of the parameters are given in Table 1.

S_0	$\gamma = 0$	$\gamma = 0.25$	$\gamma = 0.5$	$\gamma = 0.75$
3	$c^* \approx 2.1$	$c^* \approx 1.75$	$c^* \approx 1.16$	$c^* \approx 0.23$
5	$c^* \approx 2.6$	$c^* \approx 2.1$	$c^* \approx 1.5$	$c^* \approx 0.52$
7	$c^* \approx 3.1$	$c^* \approx 2.6$	$c^* \approx 1.9$	$c^* \approx 0.81$
10	$c^* \approx 3.5$	$c^* \approx 3$	$c^* \approx 2.6$	$c^* \approx 1.9$

Table 4. Calculated c^* [km/week] at different values of η without quarantine and $S_0 = 10$.

η	c^*
0.4	$c^* \approx 2.9$
0.5	$c^* \approx 3.38$
0.59	$c^* \approx 3.5$
0.65	$c^* \approx 3.88$
0.7	$c^* \approx 4$

Table 5. Calculated c^* [km/week] at different values of ρ without quarantine and $S_0 = 10$.

ρ	c^*
2	$c^* \approx 4.7$
4	$c^* \approx 3$
6	$c^* \approx 2.1$
8	$c^* \approx 1.8$
10	$c^* \approx 1.28$
12	$c^* \approx 1.05$
14	$c^* \approx 0.87$

Table 6. Calculated c^* [km/week] at different values of q without quarantine and $S_0 = 10$.

q	c^*
0.5	$c^* \approx 4.2$
0.55	$c^* \approx 3.8$
0.6	$c^* \approx 3.75$
0.65	$c^* \approx 3.3$
0.7	$c^* \approx 3.28$

Table 7. Summary of COVID-19 spreading speeds for $\gamma = 0$.

Parameter	c^* [km/week]
$S_0 \in [3, 10]$	$c^* \in [2.1, 3.5]$
$\eta \in [0.4, 0.7]$	$c^* \in [2.9, 4]$
$\tau \in [2, 14]$	$c^* \in [4.7, 0.87]$
$q \in [0.5, 0.7]$	$c^* \in [4.2, 3.28]$

Table 8. COVID-19 spreading speeds with diffusion as in [1].

S_0	c^* [km/week]
3	$c^* \approx 14$
4	$c^* \approx 16.4$
5	$c^* \approx 18.6$
6	$c^* \approx 19.9$

We conclude this work by pointing out some of the limitations of the model and future study. The model assumes that the recovered individuals are immune to the disease. Hence, the resulting system is a susceptible-exposed(infected)-infectious-recovered (SEIR) mathematical model. However, allowing recovered people to return to the susceptible stage seems reasonable biologically. With this assumption, we would have a more complex mathematical model. This fact compels us to extend this work in the future by studying the SEIRS version of this model.

Use of AI tools declaration

The authors declares he has not used Artificial Intelligence (AI) tools in the creation of this article.

Acknowledgments

The author extends his appreciation to the Deanship of Scientific Research at Northern Border University, Arar, KSA, for funding this research work through the project number NBU-FPEJ-2024-133-01.

Conflict of interest

The author declares no conflict of interest.

References

1. K. M. Alanazi, Modeling and simulating an epidemic in two dimensions with an application regarding COVID-19, *Computation*, **12** (2024), 34. https://doi.org/10.3390/computation12020034
2. K. M. Alanazi, Z. Jackiewicz, H. R. Thieme, Numerical simulations of spread of rabies in a spatially distributed fox population, *Math. Comput. Simul.*, **159** (2019), 161–182. https://doi.org/10.1016/j.matcom.2018.11.010
3. K. M. Alanazi, Z. Jackiewicz, H. R. Thieme, Numerical simulations of the spread of rabies in two-dimensional space, *Appl. Numer. Math.*, **135** (2019), 87–98. https://doi.org/10.1016/j.apnum.2018.08.009
4. K. M. Alanazi, Z. Jackiewicz, H. R. Thieme, Spreading speeds of rabies with territorial and diffusing rabid foxes, *Discr. Cont. Dyn. Syst. Ser. B*, **25** (2020), 2143. https://doi.org/10.3934/dcdsb.2019222
5. C. Anastassopoulou, L. Russo, L. Tsakris, C. Siettos, Modelling and forecasting of the COVID-19 outbreak, *PLoS One*, **15** (2020), e0230405. https://doi.org/10.1371/journal.pone.0230405
6. J. Arino, S. Portet, A simple model for COVID-19, *Infect. Dis. Model.*, **5** (2020), 309–315.
7. D. G. Aronson, The asymptotic speed of propagation of a simple epidemic, *Nonlinear Diffus.*, **14**, (1977), 1–23.
8. D. G. Aronson, H. F. Weinberger, Nonlinear diffusion in population genetics, combustion, and nerve pulse propagation, *Partial Differ. Equ. Related Topics*, **446**, (1975), 5–49.

9. D. G. Aronson, H. F. Weinberger, Multidimensional nonlinear diffusion arising in population genetics, *Adv. Math.*, **30** (1978), 33–76. https://doi.org/10.1016/0001-8708(78)90130-5

10. A. Babaei, M. Ahmadi, H. Jafari, A. Liya, A mathematical model to examine the effect of quarantine on the spread of coronavirus, *Chaos Solitons Fract.*, **142** (2021), 110418. https://doi.org/10.1016/j.chaos.2020.110418

11. B. Batista, Minimizing disease spread on a quarantined cruise ship: a model of COVID-19 with asymptomatic infections, *Math. Biosci.*, **329** (2020), 108442. https://doi.org/10.1016/j.mbs.2020.108442

12. H. Berestycki, J. M. Roquejoffre, L. Rossi, Propagation of epidemics along lines with fast diffusion, *Bull. Math. Biol.*, **83** (2021), 2. https://doi.org/10.1007/s11538-020-00826-8

13. J. Chen, Pathogenicity and transmissibility of 2019-nCoV-a quick overview and comparison with other emerging viruses, *Microbes Infect.*, **22** (2020), 69–71. https://doi.org/10.1016/j.micinf.2020.01.004

14. Q. Cui, Z. Hu, Y. Li, J. Han, Z. Teng, J. Qian, Dynamic variations of the COVID-19 disease at different quarantine strategies in Wuhan and mainland China, *J. Infect. Publ. Heal.*, **13** (2020), 849–855. https://doi.org/10.1016/j.jiph.2020.05.014

15. O. Diekmann, Limiting behaviour in an epidemic model, *Nonlinear Anal.*, **1** (1977), 459–470.

16. O. Diekmann, Thresholds and travelling waves for the geographical spread of infection, *J. Math. Biol.*, **6** (1978), 109–130. https://doi.org/10.1007/BF02450783

17. O. Diekmann, Run for your life. A note on the asymptotic speed of propagation of an epidemic, *J. Diff. Equ.*, **33** (1979), 5873. https://doi.org/10.1016/0022-0396(79)90080-9

18. R. Engbert, M. M. Rabe, R. Kliegl, S. Reich, Sequential data assimilation of the stochastic SEIR epidemic model for regional COVID-19 dynamics, *Bull. Math. Biol.*, **83** (2021), 1. https://doi.org/10.1007/s11538-020-00834-8

19. Y. Feng, Q. Li, X. Tong, R. Wang, S. Zhai, C. Gao, et al., Spatiotemporal spread pattern of the COVID-19 cases in China, *PLoS One*, **15** (2020), e0244351. https://doi.org/10.1371/journal.pone.0244351

20. M. Gatto, E. Bertuzzo, L. Mari, S. Miccoli, L. Carraro, R. Casagrandi, et al., Spread and dynamics of the COVID-19 epidemic in Italy: effects of emergency containment measures, *Proc. Natl. Academy Sci.*, **117** (2020), 10484–10491. https://doi.org/10.1073/pnas.2004978117

21. Y. Guo, T. Li, Modeling the competitive transmission of the Omicron strain and Delta strain of COVID-19, *J. Math. Anal. Appl.*, **526** (2023), 127283. https://doi.org/10.1016/j.jmaa.2023.127283

22. J. Hellewell, S. Abbott, A. Gimma, N. I. Bosse, C. I Jarvis, T. W. Russell, et al., Feasibility of controlling COVID-19 outbreaks by isolation of cases and contacts, *Lancet Global Heal.*, **8** (2020), e488–e496. https://doi.org/10.1016/S2214-109X(20)30074-7

23. C. Hou, J. Chen, Y. Zhou, L. Hua, J. Yuan, S. He, et al., The effectiveness of quarantine of Wuhan city against the Corona Virus Disease 2019 (COVID-19): a well-mixed SEIR model analysis, *J. Medical Virol.*, **92** (2020), 841–848. https://doi.org/10.1002/jmv.25827

24. K. K. Hwang, C. J. Edholm, O. Saucedo, L. J. S. Allen, N. Shakiba, A hybrid epidemic model to explore stochasticity in COVID-19 dynamics, *Bull. Math. Biol.*, **84** (2022), 91. https://doi.org/10.1007/s11538-022-01030-6
25. E. Iboi, O. O. Sharomi, C. Ngonghala, A. B. Gumel, Mathematical modeling and analysis of COVID-19 pandemic in Nigeria, *Math. Biosci. Eng.*, **17** (2020), 7192–7220. https://doi.org/10.3934/mbe.2020369
26. A. Kouidere, L. E. Youssoufi, H. Ferjouchia, O. Balatif, M. Rachik, Optimal control of mathematical modeling of the spread of the COVID-19 pandemic with highlighting the negative impact of quarantine on diabetics people with cost-effectiveness, *Chaos Solitons Fract.*, **145** (2021), 110777. https://doi.org/10.1016/j.chaos.2021.110777
27. A. J. Kucharski, T. W. Russell, C. Diamond, Y. Liu, J. Edmunds, S. Funk, et al., Early dynamics of transmission and control of COVID-19: a mathematical modelling study, *Lancet Infect. Dis.*, **20** (2020), 553–558. https://doi.org/10.1016/S1473-3099(20)30144-4
28. Q. Li, X. Guan, P. Wu, X. Wang, L. Zhou, Y. Tong, et al., Early transmission dynamics in Wuhan, China, of novel coronavirus–infected pneumonia, *New England J. Medic.*, **382** (2020), 1199–1207. https://doi.org/10.1056/NEJMoa2001316
29. T. Li, Y. Guo, Modeling and optimal control of mutated COVID-19 (Delta strain) with imperfect vaccination, *Chaos Solitons Fract.*, **156** (2022), 111825. https://doi.org/10.1016/j.chaos.2022.111825
30. Q. Lin, S. Zhao, D. Gao, Y. Lou, S. Yang, S. S. Musa, et al., A conceptual model for the coronavirus disease 2019 (COVID-19) outbreak in Wuhan, China with individual reaction and governmental action, *Int. J. Infect. Dis.*, **93** (2020), 211–216. https://doi.org/10.1016/j.ijid.2020.02.058
31. J. M. Read, J. R. Bridgen, D. A. Cummings, A. Ho, C. P. Jewell, Novel coronavirus 2019-nCoV (COVID-19): early estimation of epidemiological parameters and epidemic size estimates, *Philos. T. Royal Soc. B*, **376** (2021), 20200265. https://doi.org/10.1098/rstb.2020.0265
32. A. Remuzzi, G. Remuzzi, COVID-19 and Italy: what next? *Lancet*, **395** (2020), 1225–1228. https://doi.org/10.1016/S0140-6736(20)30627-9
33. S. Ruan, *Spatial-Temporal Dynamics in Nonlocal Epidemiological Models,* Berlin: Springer, 2007.
34. M. A. Safi, A. B. Gumel, Dynamics of a model with quarantine-adjusted incidence and quarantine of susceptible individuals, *J. Math. Anal. Appl.*, **399** (2013), 565–575. https://doi.org/10.1016/j.jmaa.2012.10.015
35. B. Tang, F. Xia, S. Tang, N. L. Bragazzi, Q. Li, X. Sun, et al., The effectiveness of quarantine and isolation determine the trend of the COVID-19 epidemic in the final phase of the current outbreak in China, *Int. J. Infect. Dis.*, **96** (2020), 288–293. https://doi.org/10.1016/j.ijid.2020.05.113
36. J. Tanimoto, *Sociophysics Approach to Epidemics*, Singapore: Springer, 2021.
37. H. R. Thieme, A model for the spatial spread of an epidemic, *J. Math. Biol.*, **4** (1977), 337–351. https://doi.org/10.1007/BF00275082
38. H. R. Thieme, Asymptotic estimates of the solutions of nonlinear integral equations and asymptotic speeds for the spread of populations, *J. Reine Angew. Math.*, **306** (1979), 94–121. https://doi.org/10.1515/crll.1979.306.94

39. H. R. Thieme, *Mathematics in Population Biology,* Princeton: Princeton University Press, 2003.

40. H. R. Thieme, X. Q. Zhao, Asymptotic speeds of spread and traveling waves for integral equations and delayed reaction-diffusion models, *J. Diff. Equ.*, **195** (2003), 430–470. https://doi.org/10.1016/S0022-0396(03)00175-X

41. A. Viguerie, G. Lorenzo, F. Auricchio, D. Baroli, T. J. Hughes, A. Patton, et al., Simulating the spread of COVID-19 via a spatially-resolved susceptible-exposed-infected-recovered-deceased (SEIRD) model with heterogeneous diffusion, *Appl. Math. Lett.*, **111** (2021), 106617. https://doi.org/10.1016/j.aml.2020.106617

42. Y. Wang, Y. Wang, Y. Chen, Q. Qin, Unique epidemiological and clinical features of the emerging 2019 novel coronavirus pneumonia (COVID-19) implicate special control measures, *J. Medical Virol.*, **92** (2020), 568–576. https://doi.org/10.1002/jmv.25748

43. F. Wei, R. Zhou, Z. Jin, S. Huang, Z. Peng, J. Wang, et al., COVID-19 transmission driven by age-group mathematical model in Shijiazhuang City of China, *Infect. Dis. Model.*, **8** (2023), 1050–1062. https://doi.org/10.1016/j.idm.2023.08.004

44. J. T. Wu, K. Leung, G. M. Leung, Nowcasting and forecasting the potential domestic and international spread of the 2019-nCoV outbreak originating in Wuhan, China: a modelling study, *Lancet*, **395** (2020), 689–697. https://doi.org/10.1016/S0140-6736(20)30260-9

45. R. Xu, H. Rahmandad, M. Gupta, C. DiGennaro, N. Ghaffarzadegan, H. Amini, et al., Weather, air pollution, and SARS-CoV-2 transmission: a global analysis, *Lancet Planetary Heal.*, **5** (2021), e671–e680. https://doi.org/10.1016/S2542-5196(21)00202-3

46. S. Zhao, Q. Lin, J. Ran, S. S. Musa, G. Yang, W. Wang, et al., Preliminary estimation of the basic reproduction number of novel coronavirus (2019-nCoV) in China, from 2019 to 2020: a data-driven analysis in the early phase of the outbreak, *Int. J. Infect. Dis.*, **92** (2020), 214–217. https://doi.org/10.1016/j.ijid.2020.01.050

47. C. C. Zhu, J. Zhu, Dynamic analysis of a delayed COVID-19 epidemic with home quarantine in temporal-spatial heterogeneous via global exponential attractor method, *Chaos Solitons Fract.*, **143** (2021), 110546. https://doi.org/10.1016/j.chaos.2020.110546

AIMS Press